DOI: 10.1002/chem.200600205

The Preparation and Characterisation of Hetero- and Homobimetallic Complexes Containing Bridging Naphthalene-1,8-dithiolato Ligands

Stephen M. Aucott, Daniel Duerden, Yang Li, Alexandra M. Z. Slawin, and J. Derek Woollins*[a]

Abstract: Homo- and heterobimetallic complexes of the form $[(PPh_3)_2(\mu^2\text{-}1,8\text{-}S_2\text{-nap})\{ML_n\}]$ (in which (1,8-S_2-nap) = naphtho-1,8-dithiolate and $\{ML_n\}$ = $\{PtCl_2\}$ (**1**), {PtClMe} (**2**), {PtClPh} (**3**), $\{PtMe_2\}$ (**4**), $\{PtIMe_3\}$ (**5**) and $\{Mo(CO)_4\}$ (**6**)) were obtained by the addition of $[PtCl_2(NCPh)_2]$, [PtClMe(cod)] (cod = 1,5-cyclooctadiene), [PtClPh(cod)], $[PtMe_2(cod)]$, $[\{PtIMe_3\}_4]$ and $[Mo(CO)_4(nbd)]$ (nbd = norbornadiene), respectively, to $[Pt(PPh_3)_2(1,8\text{-}S_2\text{-nap})]$. Synthesis of cationic complexes was achieved by the addition of one or two equivalents of a halide abstractor, $Ag[BF_4]$ or $Ag[ClO_4]$, to $[\{Pt(\mu\text{-}Cl)(\mu\text{-}\eta^2\text{:}\eta^1\text{-}C_3H_5)\}_4]$, $[\{Pd(\mu\text{-}Cl)(\eta^3\text{-}C_3H_5)\}_2]$, $[\{IrCl(\mu\text{-}Cl)(\eta^5\text{-}C_5Me_5)\}_2]$ (in which $C_5Me_5 = Cp^* =$ 1,2,3,4,5-pentamethylcyclopentadienyl), $[\{RhCl(\mu\text{-}Cl)(\eta^5\text{-}C_5Me_5)\}_2]$, $[PtCl_2(PMe_2Ph)_2]$ and $[\{Rh(\mu\text{-}Cl)(cod)\}_2]$ to give the appropriate coordinatively unsaturated species that, upon treatment with $[(PPh_3)_2Pt(1,8\text{-}S_2\text{-nap})]$, gave complexes of the form $[(PPh_3)_2(\mu^2\text{-}1,8\text{-}S_2\text{-nap})\{ML_n\}][X]$ (in which $\{ML_n\}[X] = \{Pt(\eta^3\text{-}C_3H_5)\}[ClO_4]$ (**7**), $\{Pd(\eta^3\text{-}C_3H_5)\}[ClO_4]$ (**8**), $\{IrCl(\eta^5\text{-}C_5Me_5)\}[ClO_4]$ (**9**), $\{RhCl(\eta^5\text{-}C_5Me_5)\}[BF_4]$ (**10**), $\{Pt(PMe_2Ph)_2\}[ClO_4]_2$ (**11**), $\{Rh(cod)\}[ClO_4]$ (**12**); the carbonyl complex $\{Rh(CO)_2\}[ClO_4]$ (**13**) was formed by bubbling gaseous CO through a solution of **12**. In all cases the naphtho-1,8-dithiolate ligand acts as a bridge between two metal centres to give a four-membered $PtMS_2$ ring (M = transition metal). All compounds were characterised spectroscopically. The X-ray structures of **5**, **6**, **7**, **8**, **10** and **12** reveal a binuclear $PtMS_2$ core with Pt···M distances ranging from 2.9630(8)–3.438(1) Å for **8** and **5**, respectively. The $napS_2$ mean plane is tilted with respect to the PtP_2S_2 coordination plane, with dihedral angles in the range 49.7–76.1° and the degree of tilting being related to the Pt···M distance and the coordination number of M. The sum of the Pt(1)coordination plane/$napS_2$ angle, a, and the Pt(1)coordination plane/M(2)coordination plane angle, b, a+b, is close to 120° in nearly all cases. This suggests that electronic effects play a significant role in these binuclear systems.

Keywords: bimetallic complexes · bridging ligands · coordination compounds · crystal structure · ligand substitution

Introduction

Coordination compounds containing naphthalene-1,8-dithiolate (**A**) or the structurally related ligands naphtho[1,8-*cd*][1,8]dithiole-4,5-dithilolate (**B**), naphthalene-1,4,5,8-tetrathiolate (**C**), 3,4,7,8-tetrachloro-naptho[1,8-*cd*][1,8]dithiole-4,5-dithiolate (**D**), 2,3,4,7-tetrachloro-naphthalene-1,4,5,8-tetrathiolate (**E**) and naphthacene-5,6,11,12-tetrathiolate (**F**) are rare relative to coordination compounds containing other bidentate dithiolates, such as benzene-1,2-dithiolate or ethane-1,2-dithiolate. Teo and co-workers used oxidative addition of the proligands tetrathionaphthalene (TTN), tetrachlorotetrathionaphthalene (TCTTN) and tetrathiotetracene (TTT) to a variety of low-valent metal substrates to demonstrate the diverse structural variations obtainable from this set of ligands.[1–8] Of particular relevance to the work presented here are those compounds in which two metal centres are bridged by two sulfur atoms of the naphthalene or tetracene dithiolate ligands mentioned above, giving rise to complexes with M_2S_2 cores. For example, the tetra-iron species $[\{(CO)_3Fe\}_2(\mathbf{C})\{Fe(CO)_3\}_2]$,[2] the polymeric nickel and cobalt systems $[\{Ni\}_2(\mathbf{C})\{Ni\}_2]$,[2] $[\{(CO)_2Co\}_2(\mathbf{C})\{Co(CO)_2\}_2]$,[2] the dinuclear iridium and cobalt compounds $[\{(PPh_3)(CO)BrIr\}(\mathbf{B})\{IrBr(CO)(PPh_3)\}]$,[4] $[\{(\eta^5\text{-}C_5H_5)Co\}(\mathbf{D})\{Co(\eta^5\text{-}C_5H_5)\}]$,[7] both of which have been shown crystallographically to contain a metal–metal bond, and the nickel complex $[\{(\eta^5$-

[a] Dr. S. M. Aucott, D. Duerden, Dr. Y. Li, Prof. A. M. Z. Slawin, Prof. J. D. Woollins
Department of Chemistry, University of St Andrews
St Andrews, Fife, Scotland KY16 9ST (UK)
Fax: (+44) 1334-463384
E-mail: jdw3@st-and.ac.uk

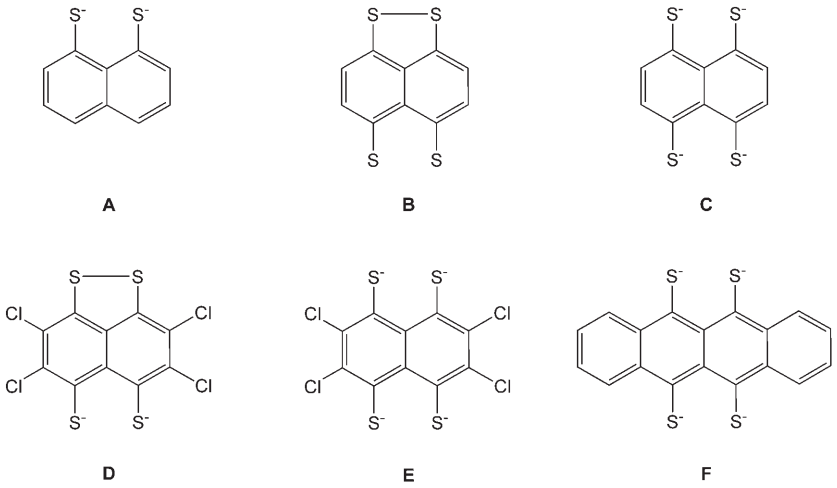

C_5H_5)Ni}(**D**){Ni(η^5-C_5H_5)}][7] containing no Ni···Ni bond. In broader terms, the synthesis and study of binuclear transition-metal complexes containing bridging dithiolate ligands has seen a recent surge of interest. Apart from the interesting structural aspects of this chemistry, much of this renewed attention is due to the generation of potentially catalytically active species. The reactivity and general properties of a metal centre may be tailored to suit a certain catalytic application by the presence of a second metal centre in close proximity to the first. In this way, a substrate molecule may react more efficiently in a cooperative manner with the two bonded or nonbonded metal centres.[9–29] We have studied sterically constrained naphthalene systems[30] and have prepared a range of compounds containing bidentate S,S ligands.[31] We recently prepared a number of dinuclear Ir(III) dimers by the oxidative addition of naphtho[1,8-*cd*]-[1,2]dithiole and related systems to [{Ir(μ-Cl)(cod)}$_2$] (cod = 1,5-cyclooctadiene), giving compounds that contain an Ir–Ir bond.[32] In addition, we have synthesised a dimeric Pt(II) compound [{(PPh$_3$)Pt(1,2-S$_2$-biphen)}$_2$] by the oxidative addition of dibenzo[1,2]dithiine to [Pt(PPh$_3$)$_4$].[33] This led us to consider the development of bimetallic systems by reaction of (readily prepared) [(PPh$_3$)$_2$Pt(μ^2-1,8-S$_2$-nap)] with suitable substrates. Here, we describe the results of studies with a range of metal fragments that illustrate the opportunities in this field. All the new complexes were fully characterised, principally by multi-element NMR spectroscopy, and in selected cases, by single-crystal X-ray diffraction studies.

Results and Discussion

Neutral complexes: [(PPh$_3$)$_2$Pt(1,8-S$_2$-nap)] was reacted with the Pt(II) precursors [PtCl$_2$(NCPh)$_2$], [PtClMe(cod)], [PtClPh(cod)] and [PtMe$_2$(cod)] (Scheme 1) at room temperature in dichloromethane, yielding [(PPh$_3$)$_2$Pt(μ^2-1,8-S$_2$-nap){PtCl$_2$}] **1**, [(PPh$_3$)$_2$Pt(μ^2-1,8-S$_2$-nap){PtClMe}] **2**, [(PPh$_3$)$_2$Pt(μ^2-1,8-S$_2$-nap){PtClPh}] **3** and [(PPh$_3$)$_2$Pt(μ^2-1,8-S$_2$-nap){PtMe$_2$}] **4**, respectively, in good-to-essentially quantitative yields (79–97%). The ^{1}H NMR spectra (Table 1) of **1**–**4** are as expected. The single methyl resonance of complex **2** appears as a broad doublet [^2J(^{1}H,^{195}Pt) = 77, ^4J(^{1}H,^{31}P) = 4 Hz] at δ(H) = 0.28 ppm (d), and the two equivalent methyl groups of complex **4** appear as a broad singlet [^2J(^{1}H,^{195}Pt) = 76 Hz] at δ(H) = −0.16 ppm (s). The ^{31}P{^{1}H} NMR spectra (Table 2) of **1** and **4** show single phosphorus environments with

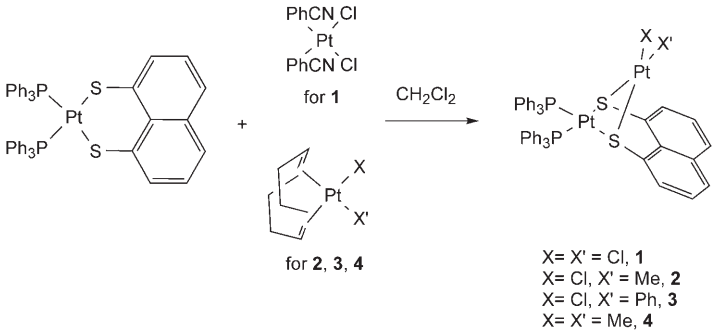

Scheme 1. Ligand-exchange reactions of Pt(II) species with [(PPh$_3$)$_2$Pt(1,8-S$_2$-nap)].

appropriate platinum satellites, whereas the spectra of **2** and **3** are the more-complex AX type. This confirms that the two platinum-bound PPh$_3$ ligands are inequivalent, with ^2J(^{31}P$_{(A)}$,^{31}P$_{(X)}$) coupling constants of 7 and 9 Hz for **2** and **3**, respectively. In both complexes there is an additional small ^3J(^{31}P$_{(X)}$,^{195}Pt) coupling constant of 61 Hz (Table 2). The IR spectra for the above complexes were mostly uninformative, though the spectrum of complex **1** shows two distinct ν(Pt–Cl) stretches at 317 and 280 cm^{-1}, which is consistent with *cis*-PtCl$_2$ geometry. For complex **1**, the positive-ion mass spectrum showed peaks centred at m/z = 1176 corresponding to $[M]^+$, as well as peaks consistent with $[M-Cl]^+$ and $[M-2Cl]^+$. The expected molecular ion in the ESI$^+$ mass spectrum for compound **2** was not observed, however, further analysis of the spectral data revealed mass peaks corresponding to $[M-Cl-Me]^+$. The fast-atom-bombardment (FAB) mass spectroscopy data for complex **3** is more conclusive and shows mass peaks for $[M]^+$, $[M-Cl]^+$, $[M-Ph]^+$ and $[M-Cl-Ph]^+$, whereas for **4**, mass peaks were observed for $[M-Me]^+$ and $[M-2Me]^+$.

The reactions of [(PPh$_3$)$_2$Pt(1,8-S$_2$-nap)] with the platinum tetramer [{PtMe$_3$I}$_4$] and [Mo(CO)$_4$(nbd)] (nbd = norbornadiene) (Scheme 2) were carried out in toluene at room temperature to give [(PPh$_3$)$_2$Pt(μ^2-1,8-S$_2$-nap){PtMe$_3$I}] **5** (94%)

Table 1. ^{1}H NMR data for complexes **1**–**13**.

Complex	^{1}H NMR data [δ in ppm]
1[a]	8.11–7.24 (m, 36H; aromatic)
2[b]	8.01–7.09 (m, 36H; aromatic), 0.28 (br d, $^2J(^1H,^{195}Pt)=77$, $^4J(^1H,^{31}P)=4$ Hz, 3H; Me)
3[a]	8.22–7.05 (m, 36H; aromatic), 6.51 (m, 5H; Ph)
4[b]	7.83–6.93 (m, 36H; aromatic), −0.15 (s, $^2J(^1H,^{195}Pt)=76$ Hz, 3H; Me)
5[b]	7.83–6.80 (m, 36H; aromatic), 1.25 (s, $^1J(^1H,^{195}Pt)=72$ Hz, 6H; 2Me), −0.11 (s, $^1J(^1H,^{195}Pt)=76$ Hz, 3H; Me)
6[b]	7.82–6.95 (m, 36H; aromatic)
7[c]	8.08–7.13 (m, 36H; aromatic); *isomer 1*: 4.91 (m, 1H; allyl), 3.93 (m, $^2J(^1H,^{195}Pt)=23$ Hz, 1H; allyl), 2.26 (m, $^2J(^1H,^{195}Pt)=69$ Hz, 2H; allyl); *isomer 2*: 4.42 (m, 2H; allyl), 3.74 (m, $^2J(^1H,^{195}Pt)=24$ Hz, 2H; allyl), 2.72 (m, $^2J(^1H,^{195}Pt)=69$ Hz, 2H; allyl)
8[b]	8.09–7.01 (m, 36H; aromatic); *isomer 1*: 5.91 (m, 1H; allyl), 4.09 (m, $J(^1H,^1H)=7$ Hz, 1H; allyl), 4.09 (d, 2H; allyl), 2.72 (d, $J(^1H,^1H)=13$ Hz, 2H; allyl); *isomer 2*: 4.91 (s, 2H; allyl), 3.96 (s, $J(^1H,^1H)=7$ Hz, 2H; allyl), 3.45 ($J(^1H,^1H)=14$ Hz)
9[b]	8.09–6.98 (m, 36H; aromatic), 0.90 (s, 15H; C_5Me_5)
10[b]	8.09–6.94 (m, 36H; aromatic), 0.97 (s, 15H; C_5Me_5)
11[b]	8.31–6.89 (m, 36H; aromatic), 1.59 (m, 12H; 4Me)
12[b]	8.11–7.05 (m, 36H; aromatic), 4.23–4.14 (br m, 4H; (cod) olefinic), 2.59–1.95 (br m, 8H; (cod) aliphatic)
13[b]	8.13–7.15 (m, 36H; aromatic)

[a] ^{1}H NMR spectra (270.2 MHz) measured in [D$_6$]DMSO. [b] ^{1}H NMR spectra (270.2 MHz) measured in $CDCl_3$. [c] ^{1}H NMR spectra (270.2 MHz) measured in CH_2Cl_2.

Table 2. ^{31}P {^{1}H} NMR data for complexes **1**–**13**.

Complex	Chemical shifts [ppm]		Coupling constants [Hz]				
	$\delta(P_X)$	$\delta(P_A)$	$^1J(^{31}P_X,^{195}Pt)$	$^1J(^{31}P_A,^{195}Pt)$	$^2J(^{31}P_X,^{31}P)$	$^2J(^{31}P_A,^{31}P)$	$^3J(^{31}P,^{195}Pt)$
1[a]	13.3	–	3552	–	–	–	–
2[b]	22.1	14.4	4000	3503	7	7	61
3[a]	18.8	14.6	3963	3507	9	9	61
4[b]	16.4	–	3256	–	–	–	–
5[b]	13.5	–	3242	–	–	–	–
6[b]	17.8	–	3103	–	–	–	–
7[c]	16.2	15.2	3202	3237	–	–	38(P_A), 42(P_X)
8[b]	18.9	17.9	3190	3196	–	–	–
9[b]	19.3	–	2559	–	–	–	–
10[b]	15.9	–	3065	–	–	–	–
11[b]	18.0	−11.2	3183	3187	–	–	–
12[b]	18.3	–	3258	–	–	–	–
13[b]	17.57	–	3272	–	–	–	–

[a] ^{31}P{^{1}H} NMR spectra (109.4 MHz) measured in [D$_6$]DMSO. [b] ^{31}P{^{1}H} NMR spectra (109.4 MHz) measured in $CDCl_3$. [c] ^{31}P{^{1}H} NMR spectra (109.4 MHz) measured in CH_2Cl_2/[D$_6$]benzene.

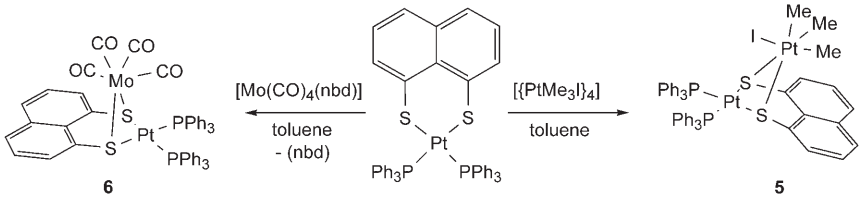

Scheme 2. Reactions of [(PPh$_3$)$_2$Pt(1,8-S$_2$-nap)] with [{PtMe$_3$I}$_4$] and [Mo(CO)$_4$(nbd)].

as a yellow powder and [(PPh$_3$)$_2$Pt(μ^2-1,8-S$_2$-nap){Mo(CO)$_4$}] **6** (95%) as bright-red crystals. The ^{1}H NMR data for **5** ($CDCl_3$) (Table 1) show the phenyl and naphthyl aromatic protons within the expected range, as well as two methyl proton environments at $\delta(H)=1.25$ [$^2J(^1H,^{195}Pt)=72$ Hz] and −0.11 ppm [$^2J(^1H,^{195}Pt)=76$ Hz] corresponding to the two axial methyl groups *trans* to the sulfur atoms of the (1,8-S$_2$-nap) ligand and one equatorial methyl group *trans* to the iodide ligand, respectively (see crystal structure, Figure 1). The ^{31}P{^{1}H} NMR ($CDCl_3$) spectrum (Table 2) has a single phosphorus environment with platinum satellites. The FAB mass spectrum of **5** showed the expected $[M]^+$ ion as well as the fragmentation peaks for $[M-Me]^+$, $[M-2Me]^+$, $[M-3Me]^+$ $[M-4Me]^+$, $[M-I]^+$ and $[M-3Me-I]^+$. Microanalytical data (Table 3) was high for both carbon and hydrogen, but following the addition of 0.5 molecules of toluene to the proposed molecular formula (used in the preparation and seen in the ^{1}H NMR spectrum), the microanalytical data were within specified limits.

The NMR and IR data for the molybdenum tetracarbonyl complex [(PPh$_3$)$_2$Pt(μ^2-1,8-S$_2$-nap){Mo(CO)$_4$}] **6** are consistent with the proposed structural assignment. In the FAB mass spectrum the expected $[M]^+$ ion and mass peaks due to the sequential loss of one, two, three and four carbonyl ligands were observed.

Mono- and dicationic complexes: Compounds [(PPh$_3$)$_2$Pt(μ^2-1,8-S$_2$-nap){Pt(η^3-C$_3$H$_5$)}][ClO$_4$] **7** and [(PPh$_3$)$_2$Pt(μ^2-1,8-S$_2$-nap){Pd(η^3-C$_3$H$_5$)}][ClO$_4$] **8** were prepared by adding the appropriate amount of halide abstractor, in this case Ag[ClO$_4$], to the metal–allyl precursors in either MeCN or a mixture of MeCN and THF. Stirring overnight in the dark gave clear, pale-yellow or colourless solutions of [M(C$_3$H$_5$)(MeCN)$_2$][ClO$_4$] (M = Pd or Pt) to which solid [(PPh$_3$)$_2$Pt(1,8-S$_2$-nap)] was added (Scheme 3). The products were isolated as pale-yellow solids in high yield (90%, **7** and 92%, **8**). The room-temperature ^{1}H NMR (CD_2Cl_2) spectrum (Table 1) of **7** shows the phenyl

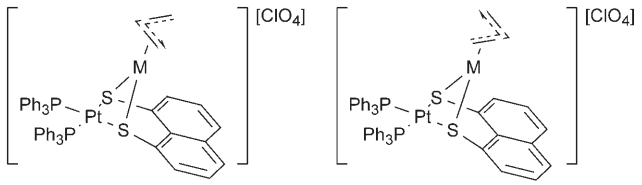

Figure 1. The two possible positional isomers of **7** and **8** that give rise to multiple NMR signals in both ^{1}H and $^{31}P\{^{1}H\}$ spectra (M = Pt or Pd).

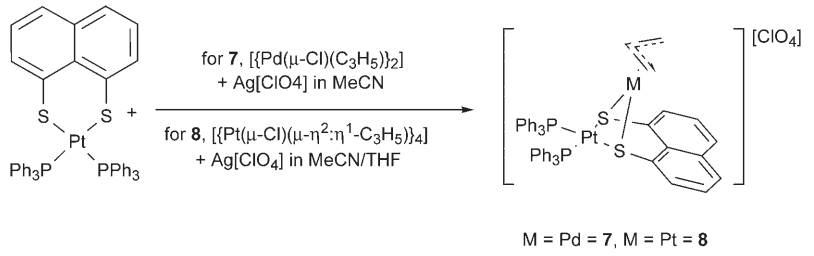

M = Pd = **7**, M = Pt = **8**

Scheme 3.

and naphthyl aromatic protons within the usual range as well as two sets of three complex multiplets for the allyl group in a ratio of approximately 2:1. The first set with the lowest intensity occurs at $\delta(H) = 4.91$, 3.93 [$^{2}J(^{1}H,^{195}Pt) = 23$ Hz] and 2.26 ppm [$^{2}J(^{1}H,^{195}Pt) = 69$ Hz]. The second set with the higher intensity in the corresponding order are observed at $\delta(H) = 4.42$, 3.74 [$^{2}J(^{1}H,^{195}Pt) = 24$ Hz] and 2.72 ppm [$^{2}J(^{1}H,^{195}Pt) = 69$ Hz]. The $^{31}P\{^{1}H\}$ NMR spectra (CH_2Cl_2/[D_6]benzene) (Table 2) of **7** consists of two singlets with two sets of platinum satellites. The resonances appears at $\delta(P) = 15.2$ [$^{1}J(^{31}P,^{195}Pt) = 3237$, $^{3}J(^{31}P,^{195}Pt) = 38$ Hz] and 16.2 ppm [$^{1}J(^{31}P,^{195}Pt) = 3202$, $^{3}J(^{31}P,^{195}Pt) = 42$ Hz]. We believe that the multiple NMR signals in both the ^{1}H and $^{31}P\{^{1}H\}$ NMR spectra are due to the orientation of the allyl group (Figure 1). Variable-temperature NMR studies of compound **7** were inconclusive because the high-boiling-point polar solvents, such as dimethyl sulfoxide and dimethyl formamide, in which **7** dissolved caused substantial decomposition and the chlorinated solvents in which **7** was readily soluble, for example, dichloromethane and chloroform, reached their boiling points before coalescence of the two positional isomers was observed. The palladium analogue [$(PPh_3)_2Pt(\mu^2$-1,8-S_2-nap){Pd(η^3-C_3H_5)}][ClO_4] **8** displayed similar NMR ($CDCl_3$) behaviour at room temperature, with two sets of three allyl resonances at $\delta(H) = 5.91$, 4.09 [$J(^{1}H,^{1}H) = 7$ Hz] and 2.72 ppm [$J(^{1}H,^{1}H) = 13$ Hz] and $\delta(H) = 4.91$, 3.96 [$J(^{1}H,^{1}H) = 7$ Hz] and 3.45 ppm [$J(^{1}H,^{1}H) = 14$ Hz]. The two singlets in the $^{31}P\{^{1}H\}$ NMR ($CDCl_3$) spectrum are displayed at $\delta(P) = 17.9$ and 18.9 ppm with $^{1}J(^{31}P,^{195}Pt)$ coupling constants of 3196 and 3190 Hz, respectively. However, for **8**, coalescence of the two positional isomers was observed in the $^{31}P\{^{1}H\}$ NMR spectra at 60 °C in [D_6]DMSO, giving rise to a single peak at $\delta(P) = 17.7$ ppm with a $^{1}J(^{31}P,^{195}Pt)$ coupling constant of 3230 Hz. Interestingly, the X-ray structures of **7** and **8** reveal the allyl group in two opposite orientations (see below), which supports our interpretation of the NMR data. Other examples of conformational or orientational isomers of palladium–allyl complexes were observed by conducting dynamic ^{1}H NMR studies of species, such as binuclear palladium–allyl complexes bearing bridging pyrazolide ligands,[46] as well as a series of bimetallic palladium/platinum complexes of the general formula [(dppe)Pd(μ-SR)$_2$M(η^3-C_3H_4R')][ClO_4] (dppe = bisdiphenylphosphinoethane, (μ-SR) = SPh, *p*-SC_6H_4Me, SEt or 1/2 $S(CH_2)_2S$, M = Pd or Pt and R′ = H or Me).[24] The positive ESI mass spectra of **7** and **8** clearly showed $[M-ClO_4]^+$ at $m/z = 1146$ and 1057, respectively.

By using a similar method to that above, [$(PPh_3)_2Pt(\mu^2$-1,8-S_2-nap){IrCl(η^5-C_5Me_5)}][ClO_4] **9** and [$(PPh_3)_2Pt(\mu^2$-1,8-S_2-nap){RhCl(η^5-C_5Me_5)}][BF_4] **10** were isolated in high yield (92%) as bright-yellow and bright-orange solids, respectively (Scheme 4). The ^{1}H NMR and $^{31}P\{^{1}H\}$ NMR

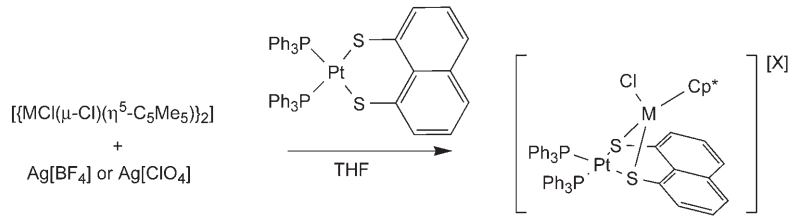

M = Ir, [ClO_4]; **9**
M = Rh, [BF_4]; **10**

Scheme 4.

($CDCl_3$) spectra (Tables 1 and 2, respectively) of compounds **9** and **10** are as anticipated.

Compounds [$(PPh_3)_2Pt(\mu^2$-1,8-S_2-nap){$Pt(PMe_2Ph)_2$}][ClO_4]$_2$ **11** (Scheme 5) and [$(PPh_3)_2Pt(\mu^2$-1,8-S_2-nap){Rh(cod)}][ClO_4] **12** (Scheme 6) were prepared analogously to the above compounds and their NMR data are summarised in Tables 1 and 2. Compound [$(PPh_3)_2Pt(\mu^2$-1,8-S_2-nap){Rh(cod)}][ClO_4] **12** was prepared as described above and as a dichloromethane solution subjected to an atmosphere of carbon monoxide gas (CO) at room temperature and pressure for 3 h, which gave a pale-orange solution. Filtration of

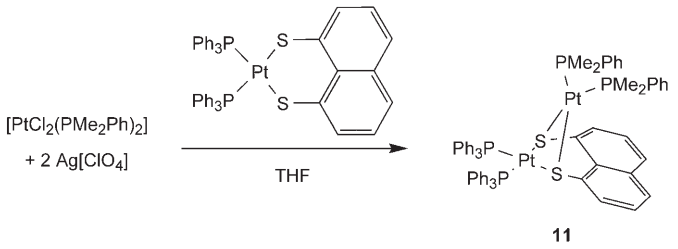

Scheme 5.

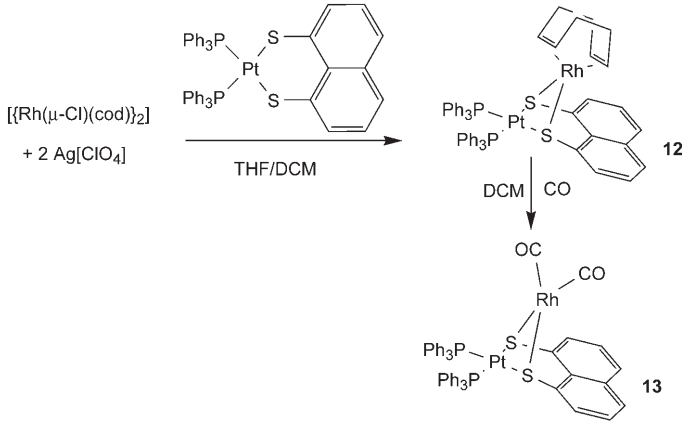

Scheme 6.

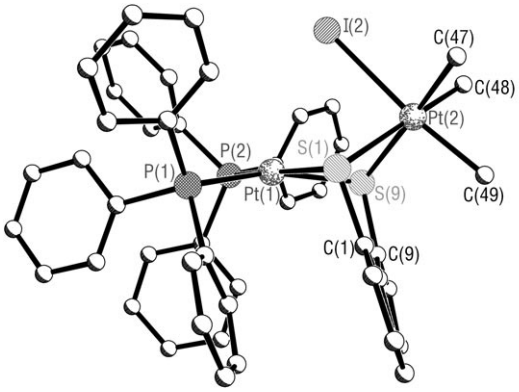

Figure 2. Crystal structure of $[(PPh_3)_2Pt(\mu^2\text{-}1,8\text{-}S_2\text{-nap})\{PtMe_3I\}]\cdot 1.5\,CHCl_3$ **5**. The $CHCl_3$ solvent molecules are omitted for clarity.

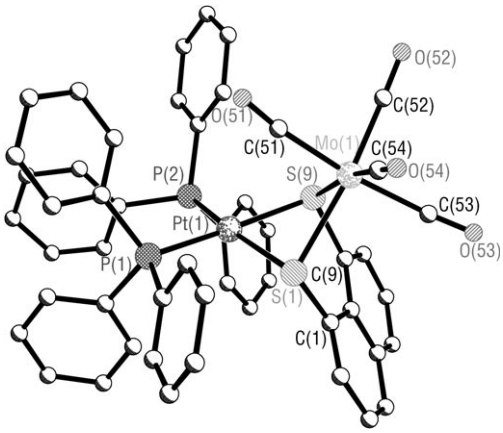

Figure 3. Crystal structure of $[(PPh_3)_2Pt(\mu^2\text{-}1,8\text{-}S_2\text{-nap})\{Mo(CO)_4\}]$ **6**.

the reaction mixture through a small Celite pad to remove a very small quantity of black precipitate, reduction of the filtrate volume, followed by the addition of hexane and a further reduction in volume yielded the dicarbonyl species $[(PPh_3)_2Pt(\mu^2\text{-}1,8\text{-}S_2\text{-nap})\{Rh(CO)_2\}][ClO_4]$ **13** (essentially quantitative yield, 99%) (Scheme 6). Microanalytical data (Table 3) for all of the complexes **1**–**13** were within specified limits for the proposed structures. IR data were as expected, revealing the appropriate vibrations due to aromatic groups and counterions.

Molecular structures: The crystal structures of **5**–**8**, **10** and **12** are shown in Figures 2–6, with selected bond lengths and angles given in Table 4. All of the structures reveal the expected square-planar geometry about Pt(1) centre, though there are some fairly large distortions that reflect the sterically demanding environments in some of the complexes. The Pt(1)–S and Pt(1)–P bond lengths lie within fairly narrow ranges [2.3549(15)–2.386(2) and 2.273(2)–2.2958(15) Å, respectively] with no special trends being evident. There is a wide variation in the Pt(1)···M distance and in the tilt or "hinge" of the $NapS_2$ ($C_{10}S_2$) mean plane with respect to the $Pt(1)S_2P_2$ mean plane. For comparison, the mononuclear complexes $[(PPh_3)_2(\mu^2\text{-}1,8\text{-}Se_2\text{-nap})]$ and $[(PMe_3)_2(\mu^2\text{-}1,8\text{-}S_2\text{-nap})]$ have tilt angles[31] of 45–50°, with the majority of the binuclear complexes reported here having larger tilting of the $napS_2$ plane from the coordination plane. There are probably two effects at work here; essentially repulsive Pt···M interaction and the

Table 3. Microanalytical data for complexes **1**–**13** (calculated values in parentheses).

	Complex	% C	% H	% S
1	$[(PPh_3)_2Pt(\mu^2\text{-}1,8\text{-}S_2\text{-nap})\{Pt(Cl)_2\}]$	47.26 (46.98)	2.57 (3.09)	5.32 (5.45)
2	$[(PPh_3)_2Pt(\mu^2\text{-}1,8\text{-}S_2\text{-nap})\{PtClMe\}]$	48.73 (48.85)	2.94 (3.40)	5.40 (5.55)
3	$[(PPh_3)_2Pt(\mu^2\text{-}1,8\text{-}S_2\text{-nap})\{PtClPh\}]$	51.72 (51.30)	3.03 (3.39)	5.11 (5.27)
4	$[(PPh_3)_2Pt(\mu^2\text{-}1,8\text{-}S_2\text{-nap})\{Pt(Me)_2\}]$	50.33 (50.79)	3.57 (3.73)	5.42 (5.65)
5	$[(PPh_3)_2Pt(\mu^2\text{-}1,8\text{-}S_2\text{-nap})\{Pt(Me)_3I\}]\cdot 0.5\,PhMe$	47.22 (47.65)	3.56 (3.74)	4.93 (4.85)
6	$[(PPh_3)_2Pt(\mu^2\text{-}1,8\text{-}S_2\text{-nap})\{Mo(CO)_4\}]$	53.28 (53.72)	2.84 (3.25)	5.80 (5.74)
7	$[(PPh_3)_2Pt(\mu^2\text{-}1,8\text{-}S_2\text{-nap})\{Pt(\eta^3\text{-}C_3H_5)\}][ClO_4]$	47.27 (47.25)	3.10 (3.32)	5.07 (5.15)
8	$[(PPh_3)_2Pt(\mu^2\text{-}1,8\text{-}S_2\text{-nap})\{Pd(\eta^3\text{-}C_3H_5)\}][ClO_4]$	50.83 (50.87)	3.36 (3.57)	5.50 (5.54)
9	$[(PPh_3)_2Pt(\mu^2\text{-}1,8\text{-}S_2\text{-nap})\{Ir(\eta^5\text{-}C_5Me_5)Cl\}][ClO_4]$	49.34 (49.01)	3.41 (3.75)	4.51 (4.67)
10	$[(PPh_3)_2Pt(\mu^2\text{-}1,8\text{-}S_2\text{-nap})\{Rh(\eta^5\text{-}C_5Me_5)Cl\}][BF_4]$	53.31 (52.95)	3.98 (4.05)	4.79 (5.05)
11	$[(PPh_3)_2Pt(\mu^2\text{-}1,8\text{-}S_2\text{-nap})\{Pt(PMe_2Ph)_2\}][ClO_4]$	46.83 (47.12)	3.47 (3.70)	3.91 (4.06)
12	$[(PPh_3)_2Pt(\mu^2\text{-}1,8\text{-}S_2\text{-nap})\{Rh(cod)\}][ClO_4]$	51.87 (52.14)	4.10 (3.96)	4.96 (5.26)
13	$[(PPh_3)_2Pt(\mu^2\text{-}1,8\text{-}S_2\text{-nap})\{Rh(CO)_2\}][ClO_4]$	49.13 (49.34)	2.90 (3.11)	5.33 (5.49)

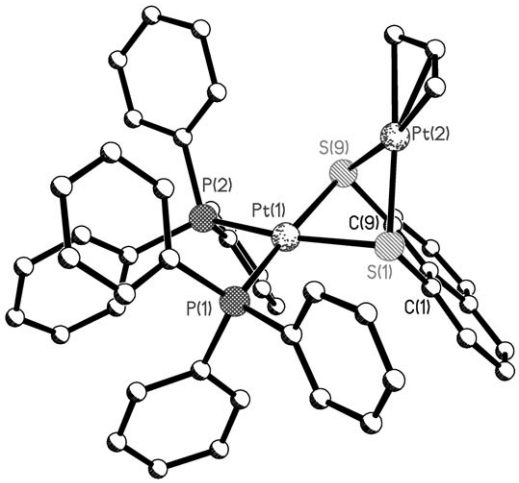

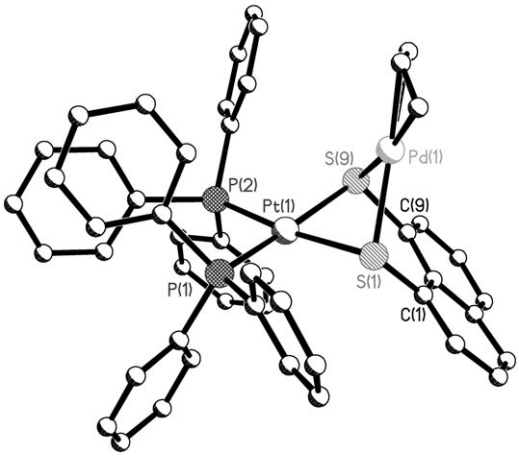

Figure 4. Crystal structure of (upper) $[(PPh_3)_2Pt(\mu^2\text{-}1,8\text{-}S_2\text{-nap})\{Pt(\eta^3\text{-}C_3H_5)\}][ClO_4]\cdot 0.5\,H_2O$ **7** and (lower) $[(PPh_3)_2Pt(\mu^2\text{-}1,8\text{-}S_2\text{-nap})\{Pd(\eta^3\text{-}C_3H_5)\}][ClO_4]\cdot CH_2Cl_2$ **8**. The solvent molecules and $[ClO_4]$ counter ions are omitted for clarity.

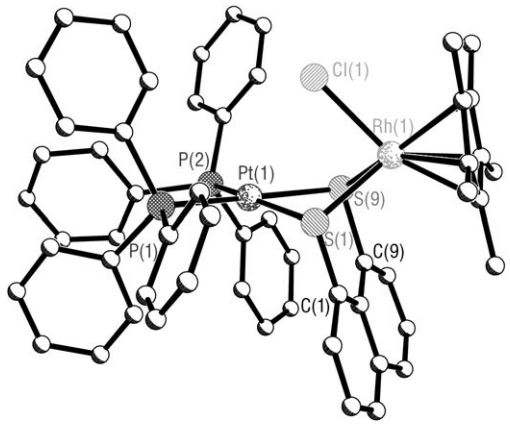

Figure 5. Crystal structure of $[(PPh_3)_2Pt(\mu^2\text{-}1,8\text{-}S_2\text{-nap})\{RhCl(\eta^5\text{-}C_5Me_5)\}][BF_4]\cdot CH_2Cl_2\cdot Et_2O$ **10**. The solvent molecules and the $[BF_4]$ counter ion are omitted for clarity.

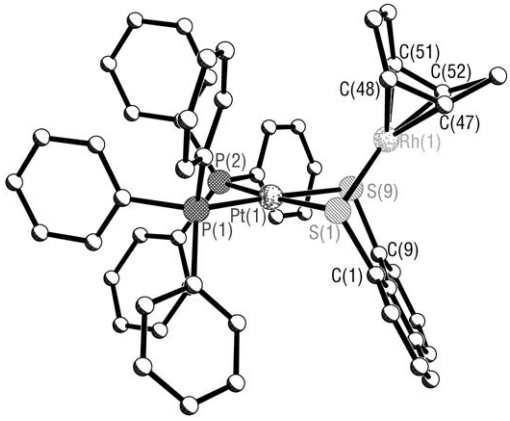

Figure 6. Crystal structure of $[(PPh_3)_2Pt(\mu^2\text{-}1,8\text{-}S_2\text{-nap})\{Rh(cod)\}][ClO_4]$ **12**. The perchlorate counterion is omitted for clarity.

steric demands of the various ligands. The observation that the mononuclear system and the binuclear Pt/Pd–allyl system **8** have similar hinge angles suggests that the orbitals on sulfur that are being used to coordinate to the second metal are not particularly stereochemically active in the mononuclear complex or, perhaps more accurately, are readily available for coordination to a second metal. It is interesting to plot the Pt(1)···M distance against the hinge angle (Figure 7), which shows a fairly good linear relationship. Compounds **5**, **6** and **10** (compounds with larger Pt(1)···M separations) appear to have larger Pt(1)···M distances than may be anticipated from extrapolation of the graph for **7**, **8** and **10**. This may be due to the higher coordination number at M in the former group imposing extra steric demands beyond the Pt···M interaction. Compound **7** has a longer Pt···Pt distance [3.1252(5) Å] than the analogous **8** [Pt···Pd of two independent molecules = 2.9817(8) and 2.9630(8) Å], which is as expected when one considers their atomic radii. Darensbourg and co-workers[47] examined the angle between the coordination planes of the two metals in $[(NiN_2S_2)W(CO)_4]$ systems and found them to be in the range 37.5–73°. In the systems described here the hinge angles of the two coordination planes are in the range 41.8–71.6°. There is a fairly linear relationship between the two sets of interplanar angles *a* and *b*, that is, as the Pt(1)coordination plane/napS_2 angle, *a*, increases the Pt(1)coordination plane/M(2)coordination plane angle, *b*, decreases. The overall consequence is that *a*+*b* is close to 120° in nearly all cases; that is, for most of the binuclear complexes studied here, the naphthalene moiety and the two metal-coordination planes are distributed equally about the central S···S vector. The exception is **10**, in which the Rh–Cl bond appears to be stereochemically active (bulky) and, thus, causes a contraction in *a*+*b*. These structural observations suggest that the majority of the systems studied here are not under steric control, the geometric features are still heavily influenced by electronic considerations about the central sulfur atoms, and the napS_2 group behaves cooperatively with the

Table 4. Bond lengths [Å] and angles [°] for complexes $[(PPh_3)_2(\mu^2\text{-}1,8\text{-}S_2\text{-nap})\{ML_n\}][X]$. Numbers in square brackets are the values for crystallographically independent molecules present in these structures.

	5	**6**	**7**	**8**	**10**	**12**
$\{ML_n\}[X]$	$\{PtIMe_3\}$	$\{Mo(CO)_4\}$	$\{Pt(\eta^3\text{-}C_3H_5)\}[ClO_4]$	$\{Pd(\eta^3\text{-}C_3H_5)\}[ClO_4]$	$\{RhCl(\eta^5\text{-}C_5Me_5)\}[BF_4]$	$\{Rh(cod)\}[ClO_4]$
Pt(1)−P(1)	2.299(2)	2.282(2)	2.281(2)	2.278(2) [2.297(2)]	2.286(3)	2.2958(15) [2.2990(16)]
Pt(1)−P(2)	2.273(2)	2.287(2)	2.292(2)	2.292(2) [2.279(2)]	2.285(3)	2.2877(17) [2.3063(14)]
Pt(1)−S(1)	2.386(2)	2.363(2)	2.364(2)	2.343(2) [2.345(2)]	2.366(3)	2.3877(17) [3.1012(5)]
Pt(1)−S(9)	2.366(2)	2.365(2)	2.382(2)	2.367(2) [2.367(2)]	2.370(3)	2.3549(15) [2.3710(17)]
C(1)−S(1)	1.757(9)	1.775(8)	1.809(9)	1.782(9) [1.793(9)]	1.748(11)	1.800(7) [1.775(7)]
C(9)−S(9)	1.782(9)	1.792(8)	1.776(8)	1.782(9) [1.775(9)]	1.800(11)	1.785(7) [1.787(7)]
S(1)···S(9)	3.06(1)	3.11(1)	3.09(1)	3.12(1) [3.12(1)]	2.98(1)	2.99(1) [3.08(1)]
M−S(1)	2.489(2)	2.564(2)	2.337(2)	2.354(2) [2.345(2)]	2.371(3)	2.3494(15) [2.3269(17)]
M−S(9)	2.430(2)	2.585(2)	2.345(2)	2.370(2) [2.367(2)]	2.376(3)	2.3380(17) [2.3544(16)]
planarity about Pt(1)	S(1) +0.121	S(1) −0.147	S(1) +0.035	S(1) +0.052 [0.038]	S(1) +0.092	S(1) −0.023 [−0.113]
	S(9) −0.172	S(9) +0.139	S(9) −0.039	S(9) −0.084 [−0.072]	S(9) −0.083	S(9) +0.017 [+0.014]
($napS_2$ to Pt)[a]	76.1	64.4	61.5	51.5 [49.7]	70.3	62.4 [58.9]
PtP_2S_2 to MS_2[b]	43.1	58.1	61.8	69.4 [71.6]	41.8	56.4 [58.0]
Sum of *a* and *b*	119.2	122.5	123.3	120.9 [121.3]	112.1	118.8 [116.9]
Pt···M	3.438(1)	3.364(1)	3.1252(5)	2.9817(8) [2.9630(8)]	3.430(1)	3.1388(5) [3.1012(5)]
P(1)-Pt-P(2)	99.42(8)	99.87(8)	98.90(7)	97.90(8) [98.23(8)]	98.73(9)	97.30(6) [97.64(5)]
S(1)-Pt-S(9)	80.09(8)	82.20(7)	81.23(8)	83.10(7) [83.04(8)]	78.06(9)	81.60(5) [81.53(5)]
S(1)-M-S(9)	76.84(7)	74.25(7)	82.59(7)	82.78(8) [82.76(8)]	77.84(10)	82.78(6) [82.40(5)]

[a] Angle between the best planes of the $C_{10}S_2$ group and the PtP_2S_2 coordination plane. [b] Angle between the $Pt(1)P_2S_2$ and MS_2 coordination planes.

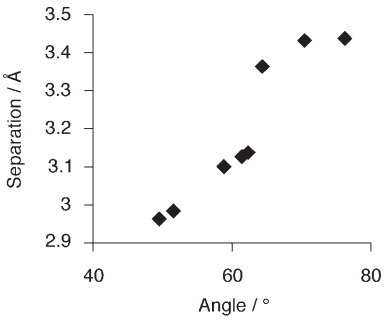

Figure 7. Plot of Pt(1)···M separation (Å) versus the angle between the $Pt(1)P_2S_2$ and $napS_2$ mean planes (°) for complexes **5**–**8**, **10** and **12**.

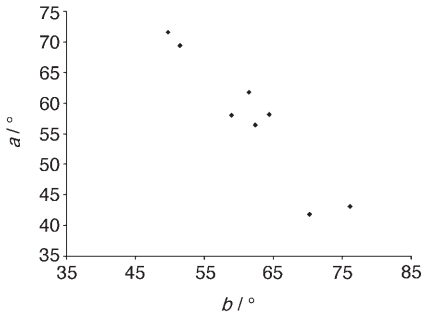

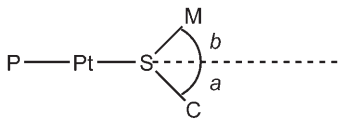

Figure 8. Top: Plot of the angle *a* between the best planes of the $C_{10}S_2$ group and the PtP_2S_2 coordination plane versus the angle *b* between the $Pt(1)P_2S_2$ and MS_2 coordination planes. Bottom: The definitions of the angles *a* and *b*.

second metal to enable the best orbital overlap of the various substituents about the sulfur atom.

As mentioned above, in **7** and **8** the allyl group has a choice of orientations, and this gives rise to dynamic NMR spectra for these compounds. The structures of **7** and **8** demonstrate elegantly (although fortuitously) this difference, revealing the two static extremes (Figure 8).

Conclusion

This work illustrates clearly the ease with which sulfur donor atoms in ligands may increase their coordination number, and suggests that M···M interactions and steric constraints on the metals fragments must be understood fully before the properties of these systems can be designed. The planar nature of the $napS_2$ ligand has allowed us to interrogate the relationship between different metric parameters and suggests that the stereochemical control of the core sulfur atoms in this and related systems must be considered carefully. This has implications in catalysis and in understanding effects in biologically relevant molecules. We anticipate that the formation of binuclear complexes from $napS_2$ could be extended to a wide range of metals and that these could provide valuable structural insights for more-complex systems.

Experimental Section

General: Unless otherwise stated, manipulations were performed under an oxygen-free nitrogen or argon atmosphere by using standard Schlenk techniques and glassware. Solvents were dried, purified and stored ac-

cording to common procedures.[34] All other reagents were purchased from Aldrich, BDH or Lancaster and were used as received, except individual starting compounds: $[Pt(Cl)_2(NCPh)_2]$,[35] [PtClMe(cod)],[36] [PtClPh(cod)],[37] $[Pt(Me)_2(cod)]$,[38] $[\{PtMe_3I\}_4]$,[39] $[Mo(CO)_4(nbd)]$,[40] $[\{Pt(\mu\text{-}Cl)(\mu\text{-}\eta^2\text{:}\eta^1\text{-}C_3H_5)\}_4]$,[41] $[\{Pd(\mu\text{-}Cl)(\eta^3\text{-}C_3H_5)\}_2]$,[42] $[\{IrCl(\mu\text{-}Cl)(\eta^5\text{-}C_5Me_5)\}_2]$,[43] $[\{RhCl(\mu\text{-}Cl)(\eta^5\text{-}C_5Me_5)\}_2]$,[43] *cis*-$[PtCl_2(PMe_2Ph)]$,[44] $[\{Rh(\mu\text{-}Cl)(cod)\}_2]$[45] and $[(PPh_3)_2Pt(\mu^2\text{-}1,8\text{-}S_2\text{-}nap)]$.[30] The ^{31}P and ^1H NMR spectra were recorded by using a Jeol GSX 270MHz spectrometer. The IR spectra (KBr discs) were recorded by using a Perkin–Elmer System 2000 FTIR spectrophotometer. Microanalyses were performed by the St Andrews University service within this Department. FAB and EI mass spectrometry was performed by the Swansea Mass Spectrometer Service.

$[(PPh_3)_2Pt(\mu^2\text{-}1,8\text{-}S_2\text{-}nap)\{PtCl_2\}]$ 1: $[PtCl_2(NCPh)_2]$ (0.078 g, 0.165 mmol) was added as a solid in a single portion to a stirred solution of $[(PPh_3)_2Pt(1,8\text{-}S_2\text{-}nap)]$ (0.150 g, 0.165 mmol) in dichloromethane (10 cm^3). After 30 min of stirring a yellow solid started to precipitate from the clear, yellow solution. Stirring was continued for a further 5 h and the yellow solid was collected by suction filtration, washed with dichloromethane (3 cm^3) and then diethyl ether (2×10 cm^3) and then dried in vacuo overnight. Yield: 0.179 g, 92%; FAB^+ MS: *m/z*: 1176 $[M]^+$, 1140 $[M-Cl]^+$, 1106 $[M-2Cl]^+$.

$[(PPh_3)_2Pt(\mu^2\text{-}1,8\text{-}S_2\text{-}nap)\{PtClMe\}]$ 2: This was prepared in the same manner as compound **1** by using $[(PPh_3)_2Pt(1,8\text{-}S_2\text{-}nap)]$ (0.100 g, 0.11 mmol) and [PtClMe(cod)] (0.039 g, 0.11 mmol). The mixture was stirred for 45 min to give a yellow solution. After heating briefly to reflux and cooling, the mixture was stirred for a further 2 h to give a dark-orange solution. A yellow solid was precipitated from the reaction mixture by the dropwise addition of hexane (10 cm^3), this material was collected by suction filtration, washed with hexane (2×10 cm^3) and dried in vacuo. Yield: 0.123 g, 97%; ESI^+ MS: *m/z*: 1140 $[M-Me]^+$, 1105 $[M-Me-Cl]^+$.

$[(PPh_3)_2Pt(\mu^2\text{-}1,8\text{-}S_2\text{-}nap)\{PtClPh\}]$ 3: This was prepared in the same manner as compound **2** by using $[(PPh_3)_2Pt(1,8\text{-}S_2\text{-}nap)]$ (0.102 g, 0.11 mmol) in dicholoromethane (10 cm^3) and [PtClPh(cod)] (0.047 g, 0.11 mmol). Yield: 0.111 g, 82%; FAB^+ MS: *m/z*: 1217 $[M]^+$, 1140 $[M-Ph]^+$, 1105 $[M-Ph-Cl]^+$.

$[(PPh_3)_2Pt(\mu^2\text{-}1,8\text{-}S_2\text{-}nap)\{PtMe_2\}]$ 4: This was prepared in the same manner as compound **1** by using $[(PPh_3)_2Pt(1,8\text{-}S_2\text{-}nap)]$ (0.101 g, 0.11 mmol) and $[PtMe_2(cod)]$ (0.037 g, 0.11 mmol). The mixture was stirred for a total of 3 h to give an orange solution. Yield: 0.099 g, 79%; FAB^+ MS: *m/z*: 1119 $[M-Me]^+$, 1104 $[M-2Me]^+$.

$[(PPh_3)_2Pt(\mu^2\text{-}1,8\text{-}S_2\text{-}nap)\{PtMe_3I\}]$ 5: $[\{PtMe_3I\}_4]$ (0.060 g, 0.16 mmol) was added in one portion to a stirred solution of $[(PPh_3)_2Pt(1,8\text{-}S_2\text{-}nap)]$ (0.150 g, 0.16 mmol) in toluene (10 cm^3). The mixture was stirred for 60 min to give a dark-orange solution. After stirring for a further 3 h the solution became pale yellow. The reaction mixture was reduced in volume to ca. 3 cm^3 under reduced pressure, hexane (20 cm^3) was then added to the stirred reaction mixture to precipitate a bright-yellow solid. This material was collected by suction filtration, washed with hexane (2× 10 cm^3) and dried in vacuo. Yield: 0.198 g, 94%; FAB^+ MS: *m/z*: 1277 $[M]^+$, 1262 $[M-Me]^+$, 1247 $[M-2Me]^+$, 1232 $[M-3Me]^+$ 1217 $[M-4Me]^+$, 1151 $[M-I]^+$ and 1105 $[M-3Me-I]^+$.

$[(PPh_3)_2Pt(\mu^2\text{-}1,8\text{-}S_2\text{-}nap)\{Mo(CO)_4\}]$ 6: $[Mo(CO)_4(nbd)]$ (0.054 g, 0.18 mmol) was added in one portion to a stirred solution of $[(PPh_3)_2Pt(1,8\text{-}S_2\text{-}nap)]$ (0.149 g, 0.16 mmol) in toluene (20 cm^3). The mixture was stirred for 60 min to give a dark-red solution. After stirring for a further 3 h a red precipitate started to form, the mixture was stirred for a total of 18 h. The reaction mixture was heated to approximately 70°C to redissolve the precipitate before filtration through a Celite plug to remove a small quantity of black insoluble material. Toluene (2×10 cm^3) was used to wash the Celite until the washings were colourless. The red filtrate was stored at −14°C overnight and the resulting red crystalline material was collected by suction filtration, washed with hexane (2× 10 cm^3) and dried in vacuo. Yield: 0.174 g, 95%; IR (KBr): $\tilde{\nu}(CO) = 2003$ (vs), 1894 (s), 1862 (s), 1833 cm^{-1} (s); FAB^+ MS: *m/z*: 1118 $[M]^+$, 1090 $[M-CO]^+$, 1062 $[M-2CO]^+$, 1034 $[M-3CO]^+$ 1006 $[M-4CO]^+$.

$[(PPh_3)_2Pt(\mu^2\text{-}1,8\text{-}S_2\text{-}nap)\{Pt(\eta^3\text{-}C_3H_5)\}][ClO_4]$ 7: $[\{Pt(\mu\text{-}Cl)(\mu\text{-}\eta^2\text{:}\eta^1\text{-}C_3H_5)\}_4]$ (0.049 g, 0.045 mmol) was added in one portion to a stirred solution of $Ag[ClO_4]$ (0.038 g, 0.18 mmol) in a mixture of acetonitrile (15 cm^3) and THF (15 cm^3). The mixture was stirred in the dark for 24 h to give a yellow solution. Solid $[(PPh_3)_2Pt(1,8\text{-}S_2\text{-}nap)]$ (0.167 g, 0.18 mmol) was added in one portion to give a very pale-yellow solution with a colourless suspension. The reaction mixture was stirred for a further 60 min before being filtered through a Celite plug to remove the precipitated AgCl, and was subsequently washed through with THF (2× 10 cm^3). The yellow filtrate was evaporated to ca. 5 cm^3 under reduced pressure and the product was precipitated by the addition of diethyl ether (30 cm^3). The yellow powder was collected by suction filtration, washed with diethyl ether (2×10 cm^3) and dried overnight in vacuo. Yield: 0.205 g, 90%; MS: *m/z*: 1145 $[M-ClO_4]^+$, 1105 $[M-ClO_4-C_3H_5]^+$.

$[(PPh_3)_2Pt(\mu^2\text{-}1,8\text{-}S_2\text{-}nap)\{Pd(\eta^3\text{-}C_3H_5)\}][ClO_4]$ 8: This was prepared in a similar fashion to **7**. Yield: 0.186 g, 95%; ESI MS: *m/z*: 1057 $[M-ClO_4]^+$.

$[(PPh_3)_2Pt(\mu^2\text{-}1,8\text{-}S_2\text{-}nap)\{Ir(\eta^5\text{-}C_5Me_5)Cl\}][ClO_4]$ 9: This was prepared in a similar fashion to **7** by using $[\{IrCl(\mu\text{-}Cl)(\eta^5\text{-}C_5Me_5)\}_2]$ (0.073 g, 0.09 mmol). Yield: 0.232 g, 92%; ESI MS: *m/z*: 1273 $[M-ClO_4]^+$, 1011 $[M-ClO_4-PPh_3]^+$, 975 $[M-ClO_4-Cl-PPh_3]^+$.

Table 5. Crystallographic data for complexes **5**–**8**, **10** and **12**.

	5	**6**	**7**	**8**	**10**	**12**
formula	$C_{49}H_{45}IP_2Pt_2S_2\cdot 1.5\,CHCl_3$	$C_{50}H_{36}MoO_4P_2PtS_2\cdot 1.5\,C_7H_8\cdot C_2H_3N$	$C_{49}H_{41}P_2Pt_2S_2\cdot ClO_4\cdot 0.5\,H_2O$	$C_{49}H_{41}ClO_4P_2PdPtS_2\cdot CH_2Cl_2\cdot C_4H_{10}O\cdot 0.5\,H_2O\cdot 0.25\,CH_4O$	$C_{56}H_{51}BClF_4P_2PtRhS_2\cdot CH_2Cl_2\cdot C_4H_{10}O$	$C_{54}H_{48}P_2PtRhS_2\cdot ClO_4$
diffractometer/*T* [K]	Smart/125	Smart/125	Smart/125	Mercury/93	Smart/125	Mercury/93
M_r	1456.04	1297.13	1254.52	1253.36	1429.33	1220.43
crystal system	monoclinic	triclinic	orthorhombic	triclinic	triclinic	monoclinic
space group	*P*2(1)/*n*	*P*$\bar{1}$	*Pbca*	*P*$\bar{1}$	*P*$\bar{1}$	*P*2(1)
a [Å]	10.8932(10)	12.654(3)	15.863(2)	15.2190(11)	11.001(3)	15.0777(11)
b [Å]	12.0067(11)	13.790(3)	20.611(3)	18.7733(16)	16.362(4)	15.4616(11)
c [Å]	39.946(4)	20.304(4)	27.618(4)	19.8316(17)	17.235(5)	20.6820(15)
α [°]		73.927(4)		65.635(5)	86.442(5)	
β [°]	90.294(2)	83.938(4)		74.953(5)	76.542(5)	90.4802(19)
γ [°]		65.563(4)		73.777(4)	79.274(5)	
V [Å^3]	5224.5(8)	3099.2(12)	9030(2)	4888.0(7)	2963.7(14)	4821.3(6)
Z	4	2	8	4	2	4
ρ_{calcd} [g cm^{-3}]	1.851	1.390	1.846	1.703	1.602	1.681
μ [mm^{-1}]	6.345	2.619	6.459	3.535	2.949	3.496
total reflns	30285	15692	37615	28962	14760	37530
ind. reflns	9495	8808	6476	16250	8316	17502
final *R*1/*wR*2 [$I > 2\sigma(I)$]	0.0435/0.0984	0.0486/0.1245	0.0332/0.0622	0.0535/0.1027	0.0543/0.1020	0.0313/0.0726

$[(PPh_3)_2Pt(\mu^2\text{-}1,8\text{-}S_2\text{-}nap)\{Rh(\eta^5\text{-}C_5Me_5)Cl\}][BF_4]$ 10: This was prepared in a similar fashion to **7** by using $Ag[BF_4]$ (0.032 g, 0.16 mmol) in THF (20 cm^3) and $[\{RhCl(\mu\text{-}Cl)(\eta^5\text{-}C_5Me_5)\}_2]$ (0.051 g, 0.08 mmol) in one portion. Yield: 0.192 g, 92%; ESI$^+$ MS: m/z: 1184 $[M-BF_4]^+$, 922 $[M-BF_4-PPh_3]^+$, 886 $[M-BF_4-Cl-PPh_3]^+$.

$[(PPh_3)_2Pt(\mu^2\text{-}1,8\text{-}S_2\text{-}nap)\{Pt(PMe_2Ph)_2\}][ClO_4]$ 11: This was prepared in a similar fashion to **7**. $[PtCl_2(PMe_2Ph)_2]$ (0.074 g, 0.13 mmol) was added in one portion to a stirred solution of $Ag[ClO_4]$ (0.056 g, 0.27 mmol) in THF (15 cm^3). The mixture was stirred in the dark overnight to give a colourless solution. Yield: 0.182 g, 86%; ESI MS: m/z: 1481 $[M-ClO_4]^+$, 1381 $[M-2ClO_4]^+$.

$[(PPh_3)_2Pt(\mu^2\text{-}1,8\text{-}S_2\text{-}nap)\{Rh(cod)\}][ClO_4]$ 12: This was prepared in a similar fashion to **7**. $[\{Rh(\mu\text{-}Cl)(cod)\}_2]$ (0.030 g, 0.06 mmol) was added in one portion to a stirred solution of $Ag[ClO_4]$ (0.025 g, 0.12 mmol) in THF (15 cm^3). The mixture was stirred in the dark overnight to give a yellow solution. Yield: 0.136 g, 93%; ESI MS: m/z: 1121 $[M-ClO_4]^+$, 1013 $[M-ClO_4-C_8H_{12}]^+$.

$[(PPh_3)_2Pt(\mu^2\text{-}1,8\text{-}S_2\text{-}nap)\{Rh(CO)_2\}][ClO_4]$ 13: Carbon monoxide was bubbled through a stirred dichloromethane (30 cm^3) solution of $[(PPh_3)_2Pt(\mu^2\text{-}1,8\text{-}S_2\text{-}nap)\{Rh(cod)\}]$ $[ClO_4]$ **12** (prepared as above) (0.205 g, 0.17 mmol) for 3 h to give a pale-orange solution. The volume of the reaction mixture was reduced to ca. 5 cm^3 whereupon hexane (20 cm^3) was added. The reaction mixture was reduced in volume further to ca. 15 cm^3, causing the product to precipitate as a pale-orange/yellow solid that was collected by suction filtration, washed with diethyl ether (2×10 cm^3) and dried overnight in vacuo. Yield: 0.194 g, 99%; IR (KBr): $\tilde{\nu}(CO)=2077$ (vs), 2016 cm^{-1} (vs); ESI MS: m/z: 1012 $[M-ClO_4-2CO]^+$.

Crystal-structure analyses: Single crystals of compounds **5** and **7** suitable for X-ray diffraction studies were obtained by layering a $CHCl_3$ solution with hexane; **8**, **10** and **12** were obtained by vapour diffusion of diethyl ether into CH_2Cl_2 solutions, whereas **8** was obtained from hot toluene.

Data for the X-ray characterisation experiments are given in Table 5 with bond lengths and angles in Table 4. Data were collected by using a Bruker SMART (sealed tube) system at 125 K or a Rigaku MM007 (high-brilliance rotating anode/confocal optics) Mercury ccd system working at 93 K; both using $Mo_{K\alpha}$ radiation ($\lambda=0.71073$ Å). All refinements were performed by using SHELXTL (Version 6.10, Bruker AXS, 2004). CCDC 297463–297468 contain the supplementary crystallographic data for this paper. These data can be obtained free of charge from The Cambridge Crystallographic Data Centre via www.ccdc.cam.ac.uk/data_request/cif.

[1] B. K. Teo, F. Wudl, J. H. Marshall, A. Krugger, *J. Am. Chem. Soc.* **1977**, *99*, 2349–2350.
[2] B. K. Teo, F. Wudl, J. J. Hauser, A. Krugger, *J. Am. Chem. Soc.* **1977**, *99*, 4862–4863.
[3] B. K. Teo, P. A. Snyder-Robinson, *Inorg. Chem.* **1978**, *17*, 3489–3497.
[4] B. K. Teo, P. A. Snyder-Robinson, *J. Chem. Soc. Chem. Commun.* **1979**, 255–256.
[5] B. K. Teo, P. A. Snyder-Robinson, *Inorg. Chem.* **1979**, *18*, 1490–1495.
[6] B. K. Teo, P. A. Snyder-Robinson, *Inorg. Chem.* **1981**, *20*, 4235–4239.
[7] B. K. Teo, V. Bakirtzis, P. A. Snyder-Robinson, *J. Am. Chem. Soc.* **1983**, *105*, 6330–6332.
[8] B. K. Teo, P. A. Snyder-Robinson, *Inorg. Chem.* **1984**, *23*, 32–39.
[9] D. Roundhill, *Inorg. Chem.* **1980**, *19*, 557–560.
[10] L. D. Rosenhien, J. W. McDonald, W. E. Newton, *Inorg. Chim. Acta* **1984**, *87*, L33–L35.
[11] D. O'hare, M. L. H. Green, F. G. N. Cloke, *J. Organomet. Chem.* **1985**, *282*, 225–321.
[12] E. W. Abel, N. A. Cooley, K. Kite, K. G. Orrell, V. Šik, M. B. Hursthouse, H. M. Dawes, *Polyhedron* **1987**, *6*, 1261–1272.
[13] J. Roll, H. Werner, *Inorg. Chim. Acta* **1988**, *147*, 93–97.
[14] M. Y. Darensbourg, M. Pala, S. A. Houliston, K. P. Kidwell, D. Spencer, S. S. Chojnacki, J. H. Riebenspies, *Inorg. Chem.* **1992**, *31*, 1487–1493.
[15] R. Usón, J. Forniés, M. A. Usón, S. Herrero, *J. Organomet. Chem.* **1993**, *447*, 137–144.
[16] U. Amador, E. Delgado, J. Forniés, E. Hernández, E. Lalinde, M. T. Moreno, *Inorg. Chem.* **1995**, *34*, 5279–5284.
[17] R. Xi, M. Abe, T. Susuki, T. Nishioka, K. Isobe, *J. Organomet. Chem.* **1997**, *549*, 117–125.
[18] J. Forniés-Cámer, A. M. Masdeu-Bultó, C. Claver, C. J. Cardin, *Inorg. Chem.* **1998**, *37*, 2626–2632.
[19] G. Sánchez, F. Momblona, M. Sánchez, J. Pérez, G. López, J. Casabó, E. Molins, C. Miravitlles, *Eur. J. Inorg. Chem.* **1998**, 1199–1204.
[20] M. Herberhold, G-X. Jin, A. L. Rheingold, *J. Organomet. Chem.* **1998**, *570*, 241–246.
[21] J. A. Cabeza, M. A. Martínez-García, V. Riera, D. Ardura, S. García-Granda, J. F. van der Maelen, *Eur. J. Inorg. Chem.* **1999**, 1133–1139.
[22] J. Forniés-Camer, A. M. Masdeu-Bultó, C. Claver, *Inorg. Chem. Commun.* **1999**, *2*, 89–92.
[23] N. Nakahara, M. Hirano, A. Fukuoka, S. Komiya, *J. Organomet. Chem.* **1999**, *572*, 81–85.
[24] J. Ruiz, J. Giner, V. Rodríguez, G. López, J. Casabó, E. Molins, C. Miravitlles, *Polyhedron* **2000**, *19*, 1627–1631.
[25] E. Erkizia, R. R. Conry, *Inorg. Chem.* **2000**, *39*, 1674–1679.
[26] W. Su, R. Cao, M. Hong, D. Wu, J. Lu, *J. Chem. Soc. Dalton Trans.* **2000**, 1527–1532.
[27] N. K. Kiriakidou-Kazemifar, M. Haukka, T. A. Pakkanen, S. P. Tunik, E. Nordlander, *J. Organomet. Chem.* **2001**, *623*, 65–73.
[28] A. R. Dias, M. H. Garcia, M. J. Villa de Brito, A. Galvão, *J. Organomet. Chem.* **2001**, *632*, 75–84.
[29] J. Forniés-Cámer, C. Claver, A. M. Masdeu-Bultó, C. J. Cardin, *J. Organomet. Chem.* **2002**, *662*, 188–191; J. Forniés-Cámer, A. M. Masdeu-Bultó, C. Claver, *Organometallics* **2002**, *21*, 2609–2618.
[30] P. Kilian, D. Philp, A. M. Z. Slawin, J. D. Woollins, *Eur. J. Inorg. Chem.* **2003**, 249–254; P. Kilian, A. M. Z. Slawin, J. D. Woollins, *Chem. Eur. J.* **2003**, *9*, 215–222; P. Kilian, A. M. Z. Slawin, J. D. Woollins, *Chem. Commun.* **2003**, 1174–1175; P. Kilian, A. M. Z. Slawin, J. D. Woollins, *Dalton Trans.* **2003**, 3876–3885; P. Kilian, H. L. Milton, A. M. Z. Slawin, J. D. Woollins, *Inorg. Chem.* **2004**, *43*, 2252–2260; P. Kilian, A. M. Z. Slawin, J. D. Woollins, *Inorg. Chim. Acta* **2005**, *358*, 1719–1723.
[31] S. M. Aucott, H. L. Milton, S. D. Robertson, A. M. Z. Slawin, G. D. Walker, J. D. Woollins, *Chem. Eur. J.* **2004**, *10*, 1666–1676; S. D. Robertson, S. M. Aucott, C. J. Burchell, H. L. Milton, A. M. Z. Slawin, J. D. Woollins, *Phosphorus Sulfur Silicon Relat. Elem.* **2004**, *179*, 987–988; S. M. Aucott, H. L. Milton, S. D. Robertson, A. M. Z. Slawin, J. D. Woollins, *Heteroat. Chem.* **2004**, *15*, 531–542; S. M. Aucott, P. Kilian, H. L. Milton, S. D. Robertson, A. M. Z. Slawin, J. D. Woollins, *Inorg. Chem.* **2005**, *44*, 2710–2718; S. M. Aucott, P. Kilian, S. D. Robertson, A. M. Z. Slawin, J. D. Woollins, *Chem. Eur. J.* **2006**, *12*, 895–902; S. D. Robertson, A. M. Z. Slawin, J. D. Woollins, *Polyhedron* **2006**, *25*, 823–826.
[32] S. M. Aucott, H. L. Milton, S. D. Robertson, A. M. Z. Slawin, J. D. Woollins, *Dalton Trans.* **2004**, 3347–3352.
[33] S. M. Aucott, P. Kilian, S. D. Robertson, A. M. Z. Slawin, J. D. Woollins, *Chem. Eur. J.* **2006**, *12*, 895–902.
[34] D. Perrin, W. L. F. Armarego, *Purification of Laboratory Chemicals*, 3rd ed., Pergamon Press, Oxford, **1988**.
[35] A. B. Goel, S. Goel, H. C. Clark, *Synth. React. Inorg. Met.-Org. Chem.* **1981**, *11*, 289–298.
[36] H. C. Clark, L. E. Manzer, *J. Organomet. Chem.* **1973**, *59*, 411–428.
[37] C. Eaborn, K. J. Odell, A. Pidcock, *J. Chem. Soc. Dalton Trans.* **1978**, 357–369.
[38] E. Costa, P. G. Pringle, M. Ravetz, *Inorg. Synth.* **1997**, *31*, 248–292.
[39] J. C. Baldwin, W. C. Kasaka, *Inorg. Chem.* **1975**, *14*, 2020–2020.

[40] M. Y. Darensbourg, M. Pala, S. A. Houliston, K. P. Kidwell, D. Spencer, S. S. Chojnacki, J. H. Reibenspies, *Inorg. Chem.* **1992**, *31*, 1487–1493.
[41] J. Lukas, *Inorg. Synth.* **1974**, *15*, 75–81.
[42] A. L. Balch, L. S. Benner, *Inorg. Synth.* **1990**, *28*, 340–342.
[43] C. White, A. Yates, P. M. Maitlis, *Inorg. Synth.* **1992**, *29*, 228–234.
[44] Prepared by the addition of two equivalents of PMe_2Ph to [$PtCl_2$-(cod)] in dichloromethane.
[45] G. Giordano, R. H. Crabtree, *Inorg. Synth.* **1979**, *19*, 218–220.
[46] S. Trofimenko, *Inorg. Chem.* **1971**, *10*, 1372–1376.
[47] M. V. Rampersad, S. P. Jeffrey, M. L. Golden, J. Lee, J. H. Reibenspies, D. J. Darensbourg, M. Y. Darensbourg, *J. Am. Chem. Soc.* **2005**, *127*, 17323–17334.

Received: February 14, 2006
Published online: May 3, 2006

